JOURNAL OF SOLID STATE CHEMISTRY 108, 18–23 (1994)

The Structure and Magnetic Properties of Pr_3MO_7 with M = Nb, Ta, and Sb

J. F. Vente,* R. B. Helmholdt,† and D. J. W. IJdo*,[1]

*Gorlaeus Laboratories, Leiden University, P.O. Box 9502, 2300 RA Leiden, The Netherlands; and †Netherlands Energy Research Foundation ECN, P.O. Box 1, 1755 ZG Petten, The Netherlands

Received November 5, 1992; in revised form April 8, 1993; accepted April 13, 1993

The crystal structure of the fluorite-related praseodymium compounds with the composition Pr_3MO_7, M = Nb, Ta, and Sb, have been determined using Rietveld refinement from X-ray and neutron powder diffraction data at 293 and 4 K. The structure described is orthorhombic with space group *Cmcm* (No. 63). It is a superstructure of the cubic fluorite structure with unit cell parameters $a_{orth} \approx 2a_c$, $b_{orth} \approx c_{orth} \approx a_c\sqrt{2}$, as in La_3NbO_7. This structure consists of chains of corner linked MO_6 octahedra parallel with the c-axis. The magnetic susceptibility was measured between 4 and 300 K. The compounds obey the Curie–Weiss law including a Van Vleck temperature independent term. Pr_3SbO_7 shows a small deviation from this law below 25 K.

INTRODUCTION

Recently, the crystal structures of the compounds Nd_3RuO_7 (1) and Ln_3IrO_7 (2) have been described, having the same structure as La_3NbO_7 (3). Compounds (Ln_3MO_7) with the same structure are found for the large lanthanides and pentavalent metals with a ionic radius of around 0.7 Å. The praseodymium compounds of these series have not been investigated systematically so far. These compounds are interesting because of the ground state of Pr(III), $^3H_4$, giving in many crystals a non-Kramers doublet. This doublet has been extensively studied with electron spin resonance (ESR) and with the magnetic susceptibility. The magnetic susceptibility of Pr_2ZrS_5 reaches at low temperatures a constant value, indicating that Pr^{3+} shows the non-Kramers doublet with a nonmagnetic ground state (4). However, the two compounds which have been used most are $Pr(C_2H_5SO_4)_3 \cdot 9H_2O$ and $Pr_2B_3(NO_3)_{12} \cdot 24H_2O$, where B = Mg, Zn or a divalent transition metal ion. In the compounds mentioned the coordination sphere of Pr^{3+} is of higher symmetry than C_2, which is required for the presence of the non-Kramers doublet.

Apart from the degeneracy described above, Pr^{3+} sometimes shows a cooperative Jahn–Teller effect. As a result, the praseodymium coordination in the phase below 151 K of $PrAlO_3$ (5) is distorted. In this work, this possible distortion is studied by comparison of the praseodymium oxygen distances in the compounds Pr_3MO_7 and the lanthanide oxygen distances in the related structure Nd_3RuO_7.

The $^3H_4$ ground state of Pr^{3+} and the possible Jahn–Teller effect make a study into the structural and the magnetic properties of Pr_3MO_7 interesting. In order to study a possible structural or magnetic phase transition, the magnetic susceptibility of Pr_3NbO_7 and Pr_3TaO_7 was measured between 80 and 300 K. The structure of these two compounds has been determined from X-ray powder diffraction data at room temperature. For a more thorough investigation, Pr_3SbO_7 was chosen. The preparation of this compound is simple and Sb^{5+} is often found in regular octahedral oxygen coordination. The crystal structure of this compound has been determined at 4 K from neutron diffraction data and at 293 K from both X-ray and neutron diffraction data. The magnetic susceptibility was measured between 4 and 300 K.

As was stated in the first paragraph of this Introduction, the detailed crystal structure of the isomorphous compounds Pr_3MO_7 has not been reported so far, except the structure of Pr_3IrO_7 (2) determined on X-ray powder data only. Furthermore, the X-ray powder diffraction intensities have been published for Pr_3MO_7 with M = Nb, Ta, and Sb, without giving the correct unit cell determination (6, 7). Yokogawa *et al.* (8, 9) have given the correct space group and unit cell axis of Pr_3TaO_7.

EXPERIMENTAL

The samples Pr_3MO_7 with M = Nb, Ta, and Sb were prepared from chemically pure grade Pr_6O_{11} and Sb_2O_3, Ta_2O_5, and Nb_2O_5 respectively. Pr_6O_{11} was dried at 1000°C and left in a furnace to cool down to 200°C in order to assure stoichiometry.

[1] To whom correspondence should be addressed.

0022-4596/94 $6.00

The niobium and the tantalum compounds were prepared by firing the appropriate stoichiometric mixtures at 1250°C for 3 weeks with repeated grinding. Pr_3SbO_7 was prepared by heating the reactants at 650°C for 1 week, 800°C for 1 week, 1050°C for 4 days, and finally 1250°C for 2 days.

All reaction products were examined at room temperature with a Philips PW 1050 X-ray diffractometer using monochromated Cu$K\alpha$ radiation. The compounds were also examined with a Siemens Elmiscope 102, fitted with a 40° double tilt and lift cartridge, operating at 100 kV. In addition, the neutron powder diffraction pattern was collected for Pr_3SbO_7 at room temperature as well as at 4 K. The neutron diffraction data were collected at the Petten High Flux Reactor. The experimental details are as reported earlier (1). No precautions were taken to prevent preferred orientation. The diffraction patterns were analyzed with the Rietveld method (10). The X-ray and neutron diffraction pattern at room temperature of Pr_3SbO_7 were analyzed simultaneously. For this purpose the GSAS (version 6.2) computer program developed by Larson and Von Dreele (11) was used. In the Rietveld refinement, the first part of the diffraction patterns was excluded (up to 17° 2θ). This was done to obtain a better fit of the background function, no Bragg reflections were found in this region. The instrumental parameters refined are listed in Table 1. In the combined refinement of Pr_3SbO_7, the neutron wavelength was also refined during the initial cycles. After convergence was reached, it was kept constant. This wavelength did not differ statistically from the intended wavelength. No absorption correction was performed. The coherent scattering lengths used were Pr: 4.45 fm, Sb: 5.64 fm, and O: 5.805 fm (11). The refinements were started with the structural parameters of Nd_3RuO_7 (Groen *et al.* (1)).

The magnetic susceptibility has been measured between 80 and 300 K for all compounds studied. The measurements have been performed on a Faraday balance calibrated with dried Gd_2O_3. The magnetic susceptibility was calculated from the five fields applied (ranging from 0.3 to 1.5 T) after correction for diamagnetism by using Selwood's table (12) and for empty vessel effects. No field dependence was observed. In addition, the magnetic susceptibility for Pr_3SbO_7 has been measured down to 4 K on a SQUID with a field strength of 0.01 T. The results were fitted against the Van Vleck relation for a paramagnetic compound with a temperature independent term for the orbital magnetism:

$$\chi = \frac{C}{(T - \theta)} + \alpha, \qquad [1]$$

where

χ = the magnetic susceptibility (emu/mole Pr_3MO_7)
C = the overall Curie constant (emu · K/mole Pr_3MO_7)
T = the temperature (K)
θ = the demagnization term (K)
α = the temperature independent susceptibility (TIP) (emu/mole Pr_3MO_7).

The two curves for Pr_3SbO_7 obtained from the two apparatus do not differ statistically. From the overall Curie constant the average magnetic moment (μ) per Pr^{3+} in Pr_3MO_7 can be calculated according to:

$$\mu = \sqrt{\frac{3k}{N\beta^2} \cdot \frac{C}{3}} \cdot \mu_B \approx \sqrt{\frac{8C}{3}} \cdot \mu_B, \qquad [2]$$

where

k = Boltzmann constant
N = Avogadro's number
β = conversion factor to units of Bohr magneton
μ_B = Bohr magneton.

RESULTS

The crystal structure of the isomorphous praseodymium compounds of formula Pr_3MO_7 with M = Sb, Ta, Nb could be determined. Pr_3NbO_7 had a dark green appearance, Pr_3TaO_7 was green, and Pr_3SbO_7 showed a light gray color.

Table 1 gives the fit parameters of the compounds studied. The resulting R_{wp} of the Rietveld refinement from X-ray diffraction patterns have values well below 17%. Only Pr_3NbO_7 has a worse fit, which may be caused by the

TABLE 1
Parameters Present in the Refinements and the Fit Results

	Pr_3NbO_7 X-ray at 293 K	Pr_3TaO_7 X-ray at 293 K	Pr_3SbO_7 Neutron at 4 K	Pr_3SbO_7[a] X-ray at 293 K	Pr_3SbO_7[a] Neutron at 293 K	Pr_3SbO_7[a] Totals at 293 K
Wavelength (Å)	1.54056 1.54439	1.54056 1.54439	2.57167	1.54056 1.54439	2.57184	
2θ range (°2θ)	10–80	10–80	5–155	10–80	5–155	
Step size (°2θ)	0.1	0.1	0.1	0.1	0.1	
Background	6[b]	4[b]	4[c]	4[b]	4[b]	
Profile	4[d]	4[d]	3[e]	4[d]	4[e]	
Structure[f]	15	15	13			15
R_{wp} (%)	22.3	16.9	4.23	13.1	4.95	7.87
R_p (%)	16.4	11.1	3.27	9.69	3.89	5.38
DW-d	0.56	0.55	1.06	0.41	0.48	0.43
DW-d limits[g]	1.87 2.13	1.87 2.13	1.86 2.13			1.93 2.07
χ^2_{red}	5.97	4.93	3.53			5.66
Variables	27	25	22			35

Note. For every diffraction pattern: zero point correction, a scale factor.
[a] Combined refinement on both X-ray and neutron diffraction data.
[b] Shifted Chebyshev function of the first kind.
[c] Real space distribution function.
[d] Pseudo-Voigt profile function.
[e] Gauss (with asymmetry) profile function.
[f] Number of structural parameters (see Table 2).
[g] Lower and upper limit for the 90% confidence interval.

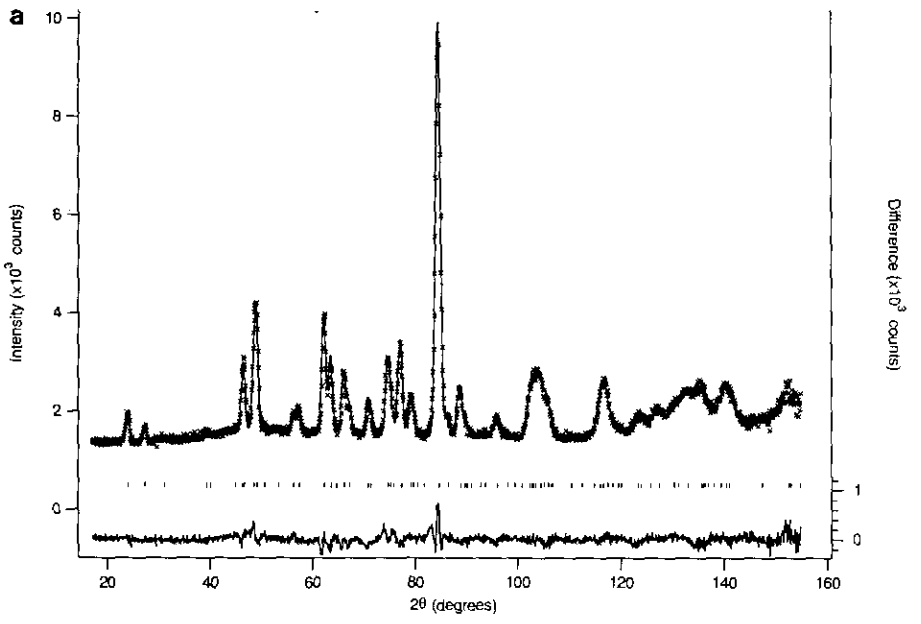

FIG. 1. (a–c) Observed (×) and calculated (full line) diffraction patterns of Pr_3SbO_7, the difference (I_{obs}–I_{calc}) curves appear at the bottom of the figures. (a) neutron diffraction pattern at 4 K, (b) neutron diffraction pattern at room temperature, and (c) X-ray diffraction pattern at room temperature.

presence of an impurity, probably $PrNbO_4$. The simultaneous refinement of the neutron and the X-ray diffraction of Pr_3SbO_7 lead to substantial lower residuals compared to the individual refinements. The total overall R_{wp} at room temperature is 7.87%, and the R_{wp} at 4 K 4.23%. Figure 1 shows the agreement between the calculated and observed intensities of Pr_3SbO_7. The results clearly indicate the compounds studied are isomorphous with Nd_3RuO_7. The DW-d values were smaller than the lower extreme of the 90% confidence interval; the estimated standard deviations are thus underestimated due to serial correlation (Hill and Flack (13)).

The space group used was *Cmcm* (No. 63) as was confirmed by the absence of specific reflections in both the X-ray and the electron diffraction patterns. Refinement in a lower space group did not lead to a better fit. Table 2 gives the results of the Rietveld refinements of the compounds studied. Selected atomic distances and angles are given in Table 3. In this table the corresponding values of Nd_3RuO_7 are given also for comparison.

In Fig. 2, the magnetic susceptibility as a function of the temperature is given for the compounds studied. This figure clearly shows the presence of a TIP. Table 4 gives the values of the fit parameters of Eq. [1] and the magnetic moment of Pr^{3+} of the compounds studied. The average magnetic moment of Pr^{3+} is $2.90\mu_B$, while the Van Vleck temperature independent term is $1.9 \cdot 10^{-3}$ emu/mole Pr_3MO_7. Pr_3SbO_7 shows below 25 K small deviations from Eq. [1].

DISCUSSION

The orthorhombic structure of Pr_3MO_7 is a superstructure of the cubic fluorite structure with space group *Cmcm* (No. 63) and unit cell parameters $a_{orth} \approx 2a_c$, $b_{orth} \approx c_{orth} \approx a_c\sqrt{2}$. The structure can be described as follows.

TABLE 2
Refined Lattice and Atomic Parameters of the Structures Studied

			Pr_3NbO_7	Pr_3TaO_7	Pr_3SbO_7 at 4 K	Pr_3SbO_7 at 293 K
Lattice parameters	a (Å)		10.959(1)	10.973(1)	10.931(1)	10.9442(6)
	b (Å)		7.5240(7)	7.5230(7)	7.5262(9)	7.5589(4)
	c (Å)		7.6676(7)	7.6721(7)	7.658(1)	7.6639(4)
Volume	Å^3		632.3(1)	633.9(1)	630.1(2)	634.01(8)
X-ray density	g cm^{-3}		4.34(1)	6.34(1)		2.84(1)
Atomic parameters[a]	Pr(1)	U_{iso} (Å^2)	0.028(3)	0.015(3)	0.44(9)	0.0111(9)
	Pr(2)	x	0.2230(4)	0.2702(4)	0.2315(6)	0.2302(1)
		y	0.2978(5)	0.2954(4)	0.2886(8)	0.2919(2)
		U_{iso} (Å^2)	0.036(1)	0.026(1)	0.44(9)	0.0126(6)
	M	U_{iso} (Å^2)	0.044(4)	0.043(3)	0.44(9)	0.0081(9)
	O(1)	x	0.098(2)	0.122(3)	0.1251(4)	0.1263(3)
		y	0.310(3)	0.306(4)	0.3150(4)	0.3144(3)
		z	0.987(3)	0.999(6)	0.9670(5)	0.9655(3)
	O(2)	x	0.175(4)	0.126(4)	0.1314(5)	0.1320(4)
		y	0.031(5)	0.030(7)	0.0259(7)	0.0229(6)
	O(3)	y	0.435(6)	0.476(9)	0.4243(8)	0.4242(6)
	O[b]	U_{iso} (Å^2)	0.032(8)	0.10(1)	0.44(9)	0.0086(7)

[a] Pr(1) at 4*a* (0,0,0); O(1) at 16 *h* (*x*,*y*,*z*); Pr(2) at 8*g* (*x*,*y*,¼); O(2) at 8*g* (*x*,*y*,¼); *M* at 4*b* (0,½,0); O(3) at 4*c* (0,*y*,¼).

[b] One U_{iso} for O(1), O(2), and O(3) and one overall U_{iso} for Pr_3SbO_7 at 4 k.

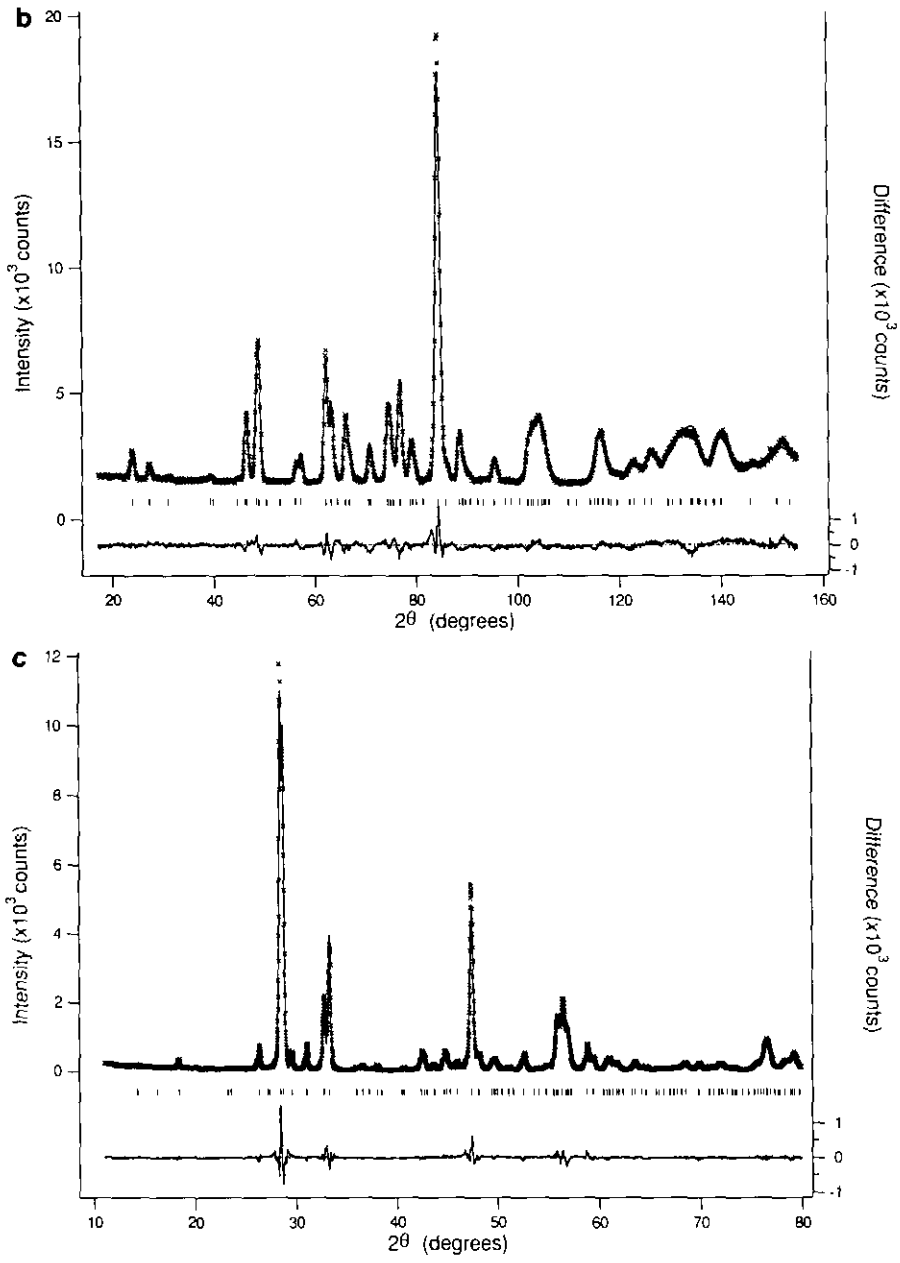

FIG. 1—*Continued*

One third of the Ln-cations are in eightfold oxygen coordination and lie in rows in the [001] direction which alternate with parallel rows of corner sharing MO_6 octahedra. The remaining two thirds are in seven coordination and lie between the slabs of the PrO_8 and the MO_6 polyhedra. The MO_6 octahedral are corner linked through the O(3) atoms. Successive O(3) atoms lie along a [001] row in zigzag sequence $(0,y,\frac{1}{4})$, $(0,-y,\frac{1}{4})$ . . . , with $y \approx 0.4$, causing a corresponding sequence of tilts to the octahedra. A drawing of this structure is given in Fig. 3.

The cell parameters of Pr_3TaO_7 were in excellent agreement with the cell axes given by Yokogawa *et al.* (8). Refinement in the space group *Pnma* (No. 62) as proposed by Yamasaki and Sugitani (14) and Peshev and Khrusanova (15) failed.

The ratio between Ln(1)–O(1) and Ln(1)–O(2), as a measure for the deformation of the Ln(1)–O(1) polyhedron, lies for the great majority of the compositions between 0.85 and 0.90, independent of the chemical composition. This Ln(1) polyhedron is almost a cube. The 7 coordination of Ln(2) is much more complicated with 5 different distances. The lengths decrease with increasing atom number of the lanthanide, in accordance with the lanthanide contraction (see, e.g., Vente and IJdo (2)).

TABLE 3
Selected Atomic Distances (Å) and Angles (°)

Distances		Pr_3NbO_7 at 293 K	Pr_3TaO_7 at 293 K	Pr_3SbO_7 at 4 K	Pr_3SbO_7 at 293 K	Nd_3RuO_7 at 293 K
Ln(1)–O(1)	4×	2.73(3)	2.67(3)	2.749(3)	2.766(2)	2.729(3)
Ln(1)–O(2)	4×	2.58(3)	2.38(3)	2.402(4)	2.407(3)	2.365(3)
Ln(2)–O(1)	2×	2.61(3)	2.52(4)	2.468(5)	2.467(3)	2.461(4)
Ln(2)–O(1)	2×	2.65(3)	2.37(4)	2.414(6)	2.420(3)	2.426(3)
Ln(2)–O(2)	1×	2.09(4)	2.55(5)	2.259(9)	2.299(4)	2.306(5)
Ln(2)–O(2)	1×	2.04(4)	2.10(5)	2.33(1)	2.318(5)	2.270(5)
Ln(2)–O(3)	1×	2.72(2)	3.26(3)	2.729(6)	2.713(2)	2.554(4)
M–O(1)	4×	1.80(3)	1.98(4)	1.968(4)	1.989(3)	1.950(3)
M–O(3)	2×	1.98(1)	1.93(1)	1.997(1)	2.002(1)	1.972(2)
Angles						
M–O(3)–*M*		151(3)	169(4)	146.9(3)	146.8(2)	143.7(3)
O(1)–*M*–O(3)		86(1)	86(2)	85.5(1)	85.7(1)	86.3(1)
O(1)–M–O(1)		72(2)	85(2)	88.0(2)	88.2(2)	89.34(9)

Note. Nd_3RuO_7 has been given for comparison (from Ref (1)).

TABLE 4
The Results of the Magnetic Susceptibility Measurements

	Pr_3NbO_7[a]	Pr_3TaO_7[a]	Pr_3SbO_7[a]	Pr_3SbO_7[b]
C(emu · K/mole)	3.14(2)	3.18(4)	3.17(9)	3.12(2)
θ (K)	−18.0(6)	−19(1)	−24(4)	−25.2(3)
α (emu · 10^3/mol)	2.14(6)	1.8(1)	1.8(2)	1.2(1)
μ Pr^{3+} (μ_B)	2.89(1)	2.91(1)	2.91(3)	2.88(1)

[a] Measured on the Faraday balance, fitted between 80 and 300 K.
[b] Measured on the SQUID, fitted between 25 and 300 K.

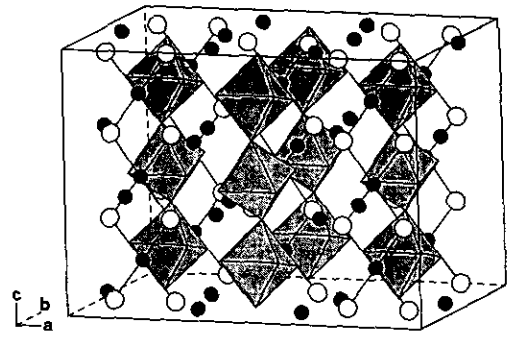

FIG. 3. The structure of Pr_3MO_7. (Pr: filled circles: O: open circles: MO_6 octahedra: shaded.)

Concluding, praseodymium causes no additional deformation, and thus no indication for a cooperative Jahn–Teller effect in these compounds has been found.

The approach for calculating the magnetic moment as given in Eq. [2] gives only an average description of the magnetic behavior of praseodymium on the two crystallographic positions. The magnetic moment of Pr^{3+}, averaged over these two crystallographic positions (see Table 2) and over the three compounds, is $2.90\mu_B$. This value is significantly smaller than the free ion value of Pr^{3+}: $g_J\sqrt{J(J+1)} = 3.58\mu_B$. This discrepancy between the measured and the free ion value, might be described to the presence of Pr^{4+}, which has a free ion

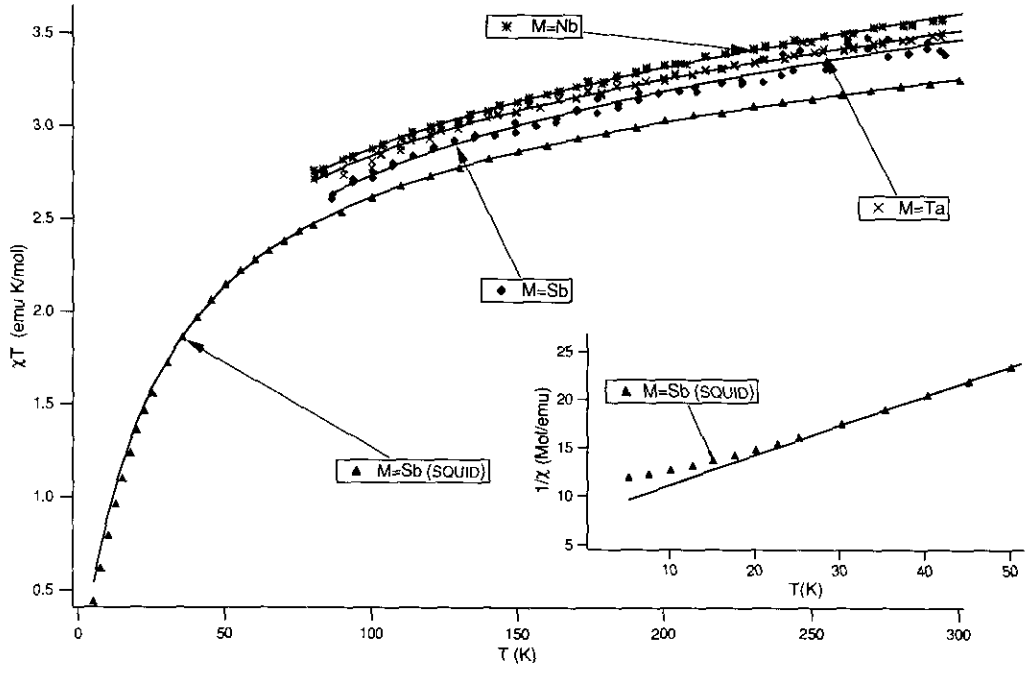

FIG. 2. The magnetic susceptibility as a function of the temperature for Pr_3MO_7. The inset shows the low temperature behavior of Pr_3SbO_7.

TABLE 5
Comparison of the Magnetic Moments Known of Pr^{3+}

Compound	μ (μ_B/mole Pr^{3+})	Range (K)	Reference
Pr_3MO_7	2.9	80–300	this work
Pr_2ZrS_5	2.6	20–250[a]	4
$Pr_2Mg_3(NO_3)_{12} \cdot 24H_2O$	2.9	1–4	16
	3.0	50–300[b]	18
	2.4	4	19
$Pr(C_2H_5SO_4)_3 \cdot 9H_2O$	3.3	100–300[b]	20
	3.4	150–300	21
$Pr_yU_{1-y}O_2$ $y = 0.01$	3.0	30–300	22
$y = 0.10$	2.8		
$PrBa_2Cu_3O_7$	2.8	100–300	17

[a] χ becomes constant at lower temperatures.
[b] at lower temperatures deviations occur.

value of $2.54\mu_B$. However, the structure determination for Pr_3SbO_7 does not indicate a nonstoichiometry. Furthermore, a compound containing both Pr^{3+} and Pr^{4+} will have a dark color, and not as light as the compounds studied. So, the possibility of the presence of Pr^{4+} can be ruled out. The value of the magnetic moment of Pr^{3+} in Pr_3MO_7 compares well to the magnetic moment in several other compounds including oxides, nitrates, sulfides, and sulfates as can be seen from Table 5. Earney *et al.* (16) have observed a Van Vleck term, with $24 \cdot 10^{-3}$ emu/mole Pr^{3+} in $Pr_2B_3(NO_3)_{12} \cdot 24H_2O$. This is an order of magnitude larger than Soderholm *et al.* (17) found in Pr $Ba_2Cu_3O_7$ ($2 \cdot 10^{-3}$ emu/mole Pr^{3+}). This study on Pr_3MO_7 yields a smaller value: $0.6 \cdot 10^{-3}$ emu/mole Pr^{3+}. This might be due to the low site symmetry of Pr^{3+} in Pr_3MO_7. Below 25 K, Pr_3SbO_7 deviates from the Curie–Weiss law in the form of a lower χ then expected on basis of the Curie–Weiss law. However, the characteristic behavior of a non-Kramers ion with a nonmagnetic ground state is not found. As a result, the $^3H_4$ ground state is likely to be split up due to the crystal field, without a degenerated level. In contrast, the non-Kramers behavior is found in $Pr_2B_3(NO_3)_{12} \cdot 24H_2O$ and also in Pr_2ZrS_5.

The TIP and the isotropic magnetic moments as presented in Table 5 are calculated from the anisotropic values as presented in the references by taking the weighted average between the in plane and the normal component of the TIP and magnetic moment.

CONCLUSIONS

A structure determination of three compounds (Pr_3MO_7, with M = Nb, Ta, and Sb) at room temperature has been given together with the structure determination of Pr_3SbO_7 at 4 K. All these compounds adopt a superstructure of the cubic fluorite structure.

Furthermore, the magnetic susceptibility of the above mentioned compounds was studied. Pr_3SbO_7 shows a small deviation from the Van Vleck behavior below 25 K. Finally, no indication for the presence of the non-Kramers doublet was observed for Pr^{3+} in these crystals.

The compounds did not show any indication of a cooperative Jahn–Teller effect; no distortions of the praseodymium polyhedra at room temperature or at 4 K were observed.

ACKNOWLEDGMENTS

The authors are indebted to Mr. G. H. Renes for the collection of the electron diffraction patterns and to Dr. J. A. M. Ruitenbeek of the Kamerlingh Onnes Laboratorium in Leiden for the measurement of the magnetic susceptibility of Pr_3SbO_7 between 4 and 300 K.

REFERENCES

1. W. A. Groen, F. P. F. van Berkel, and D. J. W. IJdo, *Acta Crystallogr. Sect. C* **43,** 2262 (1987).
2. J. F. Vente and D. J. W. IJdo *Mat. Res. Bull.* **26,** 1255 (1991).
3. H. J. Rossell, *J. Solid State Chem.* **27,** 287 (1979).
4. G. M. Nap and C. M. Plug, *Physica B* **93,** 1 (1978).
5. R. J. Birgeneau, J. K. Kjems, G. Shirane, and L. G. Van Uitert, *Phys. Rev.* **10,** 2512 (1974).
6. M. B. Varfolomeev and B. A. Narnov, *Russ. J. Inorg Chem Engl. Transl.* **23,** 955 (1978). JCPDS-file 33-1071.
7. E. P. Savchenko *et al., J. Appl. Chem.* **39,** 1797 (1966). JCPDS-file 23-515.
8. Y. Yokogawa, U. M. Yoshimura, and S. Somiya, *Solid State Ionics* **35,** 275 (1989). JCPDS-file 38-1416.
9. Y. Yokogawa, M. Yoshimura, and S. Somiya, *Solid State Ionics* **28–30,** 1250 (1988).
10. H. M. Rietveld, *J. Appl. Crystallogr. 2,* 65 (1969).
11. A. C. Larson and R. B. von Dreele," Generalized Crystal Structure Analysis System (GSAS)," Los Alamos Report LAUR 86-748, Los Alamos National Laboratory, Los Alamos.
12. P. W. Shelwood, "Magnetochemistry" 2nd ed. Interscience, New York 1956.
13. R. J. Hill and H. D. Flack, *J. Appl. Crystallogr.* **20,** 356 (1987).
14. Y. Yamasaki and Y. Sugitani, *Bull. Chem. Soc. Jpn.* **51,** 3077 (1978).
15. P. Peshev and M. Khrusanova, *Mat. Res. Bull.* **15,** 195 (1980).
16. J.J. Earney, C. P. B. Finn, and B. M. Najafabadi, *J. Phys. C: Solid State Phys.* **4,** 1013 (1971).
17. L. Soderholm, C.-K. Loong, G. L. Goodman, and B. D. Dabrowski. *Phys. Rev. B* **43,** 7923, (1991).
18. K. H. Helwege, S. H. Kahn, H. Lange, W. Rummel, W. Schembs, and B. Schneider, *Z. Phys.* **167,** 487, (1962).
19. V. E. Sells and D. Bloor, *J. Phys. C: Solid State Phys.* **9,** 379 (1976).
20. K. H. Helwege, W. Schembs, and B. Schneider, *Z. Phys.* **167,** 477, (1962).
21. J. M. Baker and B. Bleaney, *Proc. Roy. Soc. London A* **245,** 156 (1958).
22. Y. Hinatsu and T. Fujino, *J. Solid State Chem.* **74,** 163 (1988).